angles near flame arrival in the scattering volume. The bin width is ten photoelectrons and the total number of events is 1000 for each histogram. The normal shape of the histogram at 372 deg is typical of those from 300-372 and 390-420 deg. At 380 deg, early arrival of the flame causes the long tail in the distribution below the most probable density. Similarly, the distortion of the distribution to the higher density values (more photoelectrons) at 384 deg is due to late flame arrivals. This explanation of the effects of cyclic variation on the distribution justifies the attempt to separate them from the real density fluctuations.

The 382-deg histogram appears to be only slightly later than the most probable time of flame arrival. The broad, nearly constant distribution indicates that the flame front is larger than the scattering volume, i.e., thicker than 0.5 mm. This conclusion is supported by bimodal distributions at similar flame arrival times when using scattering volumes of 3-5 mm linear dimensions.

It should be noted that signal-to-noise ratios were of the order of 30:1, even when the flame was in the scattering volume. It is tempting to say the increase in fluctuations immediately behind the flame front is flame-induced turbulence; however, fast fluorescence, which the present Raman system does not discriminate against, may contribute to the signal level. Work in progress should eliminate this concern.

Acknowledgment

This work was supported by the Dept. of Energy and the Motor Vehicle Manufacturers Association.

References

[1] Setchell, R. E., "Raman Spectroscopy Measurements Within a Internal Combustion Engine," 18th Annual Rocky Mountain Spectroscopy Conference, University of Denver, Aug. 1976.

[2] Johnston, S. C., Robinson, C. W., Rorke, W. S., Smith, J. R., and Witze, P. O., "Applications of Laser Diagnostics to an Injected Engine," SAE Paper 790092, Detroit, Mich., Feb. 1979.

[3] Setchell, R. E., "Local Turbulence Properties in Flames From Time-Averaged Raman Spectroscopy Measurements," AIAA Paper 79-0087, New Orleans, La., Jan. 1979.

[4] Tomlinsen, R. G., Damon, E. K., and Buscher, H. T., "The Breakdown of Noble and Atmospheric Gases by Ruby and Neodymium Laser Pulses," *Physics of Quantum Electronics Conference Proceedings 1965*, pp. 520-526.

J80-023

Simple Analytical Modeling of Supersonic Flow around Blunt Axisymmetric Bodies

NA

D.R. Philpott*

The Hatfield Polytechnic, Hatfield, Herts, United Kingdom

20001
20017

Introduction

ALTHOUGH a number of calculation schemes are available for the supersonic blunt body problem, those methods which attempt to solve the complete inviscid equations of motion are too cumbersome for initial design studies, while simplified flow models fail to model important features such as the influence of initial blunting on afterbody pressure.

Pugh and Ward[1] attempted to model this feature by supposing that the layer of slow moving air, or entropy layer, near the body surface, which has been influenced by its passage through the near normal shock wave close to the axis of symmetry, acts like a boundary layer in providing an effective displacement surface which modifies the physical profile of the body. In the present work the same flow model is retained although the entropy layer thickness is defined more precisely and considerable differences are introduced into the calculation scheme. The proposed method thus predicts inviscid wave drag, excluding skin friction and base drag, and is likely to be suitable for initial configuration parameter studies in which economy of computation is important.

Presented as Paper 78-1356 at the AIAA Atmospheric Flight Mechanics Conference, Palo Alto, Calif., Aug. 7-9, 1978; submitted Aug. 17, 1978; revision received July 25, 1979.

Copyright © 1978 by D.R. Philpott. Published by the American Institute of Aeronautics and Astronautics, Inc., with permission.

Index categories: Supersonic and Hypersonic Flow; Aerodynamics.

*Senior Lecturer, School of Engineering.

Derivation of Drag from Shock Wave Profiles

Pugh and Ward[1] determine the wave drag of the body via Oswatitsch's theorem[2] by integrating the entropy flux cross the bow shock wave. Thus only a knowledge of the shock wave geometry is required. For the calculation the shock wave is divided into three zones (Fig. 1). Zone I is the region immediately adjacent to the axis of symmetry and is generated by the initial blunting on the body. Zone II is generated by the afterbody, and it is assumed that the flow is locally nearly conical in this region. Zone III is the far flowfield in which the shock decays to a Mach wave.

Zone I

Pugh and Ward[1] point out that frequently the problem of investigating an afterbody configuration for a particular initial blunting (e.g., spherical) arises, and in their work, as in the present method, an empirical shock wave profile is assumed in this region. However, in order to make the method more readily adaptable to different initial bluntings, an alternative simple prediction method based on Kaattaari's work[3] is currently being investigated for this zone.

Zone II

In zone II the local flow is approximated to a conical flow with a characteristic line running to b at the shock (Fig. 1) from an effective surface at δ^*. In Ref. 1 the displacement thickness of the entropy layer $o\delta^*$ is derived for a parallel afterbody, and the result scaled to account for local density changes in the nonparallel case. It is, however, possible to derive the thickness directly for the nonparallel case as follows: since the mass flow crossing the actual shock Ab and the corresponding conical shock wave ab (Fig. 1) must be equal, and taking dc along the line os

$$\int_0^b 2\pi\rho|y|u\cdot \mathrm{d}c = \int_{\delta^*}^b 2\pi\rho_c|y|u_c\cdot \mathrm{d}c \tag{1}$$

where subscript c refers to the approximate conical flow. This may be rearranged to give the mass flow in the entropy layer

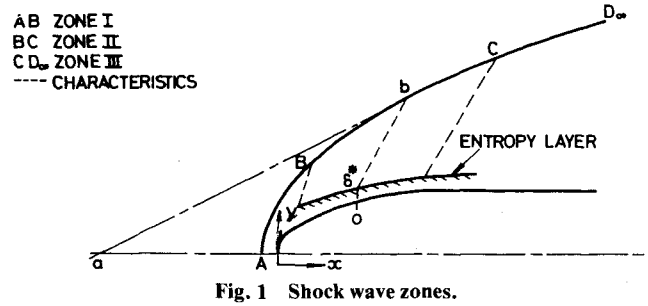

Fig. 1 Shock wave zones.

$o\delta^*$ in terms of the mass flow deficiency in the real flow along $\delta^* b$ when compared to the approximate conical flow, so that

$$\int_0^{\delta^*} 2\pi|y|u\cdot dc = \int_{\delta^*}^{b} 2\pi\rho_c\left(1-\frac{\rho|u|}{\rho_c|u_c|}\right)u_c\cdot dc \qquad (2)$$

The bracketed term in Eq. (2) may be related to the difference in entropy flux crossing $\delta^* b$ in the actual and approximate flows, and if it is assumed that this difference is small and that the bow shock wave is the only significant entropy producing mechanism, this leads to the approximate relationship[4]

$$\Delta S = \tfrac{1}{2}\{c_p[F(M_c)_{\delta^*} + F(M_c)_b] + (\Delta S_{\infty_A} - \Delta S_{\infty_b})\}\int_0^{\delta^*} 2\pi|y|\rho u\cdot dc \qquad (3)$$

where $F_{M_c} = [1+1/(\gamma-1)M_c^2]^{-1}$ and may be determined directly from the conical flow solution. ΔS_{∞_A} is the specific entropy rise across a normal shock wave and ΔS_{∞_b} that across the shock wave at b. ΔS is the difference in the total entropy flux crossing the real and conical shock waves up to point b (Fig. 1). The integral may be approximated by assuming an average value for ρu within the entropy layer. This is taken as the mean of the conical value at δ^* and the value at o which is obtained by assuming constant Mach number but allowing for the increase in stagnation entropy at the surface.

The shock wave may thus be advanced in zone II by iterating the new shock point until compatibility is obtained between the value of y_{δ^*} obtained from Eq. (3) and that given by the conical flow solution corresponding to the local slope and radius at the new point on the shock wave.

Zone III

It is assumed that the shock wave radius in zone III is sufficiently large for the profile to be insensitive to detailed body geometry. The profile in this zone is thus equivalent to that generated by a finite sharp cone with a cylindrical afterbody of the same radius as the base of the blunt body, but with the addition of the entropy layer displacement thickness. The angle of the cone is that corresponding to the shock wave slope at the last point in zone II.

The total entropy flux crossing the bow shock generated by this cone may be calculated from the pressure drag via Oswatitsch's theorem,[2] and subtraction of the entropy flux crossing the conical part of the shock wave gives the zone III contribution directly without the need for the detailed shock geometry in this region.

Discussion of Results

Figure 2 shows shock wave profiles for two spherically blunted cones at $M=2.50$ compared with "exact" calculation and experiment. The matching point between zone I and zone II was taken at the shock point, $x/r_n = 1.9$. This corresponds to the body point $x/r_n = 0.4$ and was limited by the need for a large number of steps in the region of high curvature at the nose rather than by a breakdown of the zone II flow model.

It was found that the slope of the entropy layer displacement surface near the junction of the spherical nose and conical afterbody was considerably less than the physical surface slope, which is consistent with the comparatively low surface pressures in this region. Although the entropy layer thickness is high in this region, the zone III flow model still gives an accurate estimate of the shock wave profile. Downstream of the nose the expected thinning of the entropy layer takes place as the local flow becomes progressively closer to that appropriate to a sharp cone.

Figure 3 shows the drag of a family of spherically blunted cones of $L/D=2$ for $M=2.50$. The range of the method is considerably extended compared with Pugh and Ward's results,[1] and its predicts overall drag considerably better than Newtonian theory at low d/D. At high d/D, the entropy layer thickness is high and the shock wave radius low at the end of zone II and the zone III model becomes unsatisfactory, leading to an overestimate in drag. In these circumstances it may be better to use the flow model to infer surface pressures as the zone III modeling will not then be required.

In Fig. 4 results are also given for nonspherical blunting in the form of a family of elliptically blunted cylinders. Agreement again becomes worse for the blunter cylinders, although the zone II shock wave prediction is excellent, probably for the same reason as before. Reference 4 also indicates a similar pattern of results at a higher freestream Mach number, $M=4.00$.

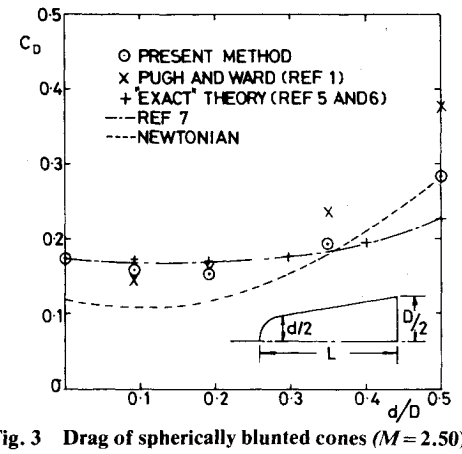

Fig. 3 Drag of spherically blunted cones ($M=2.50$).

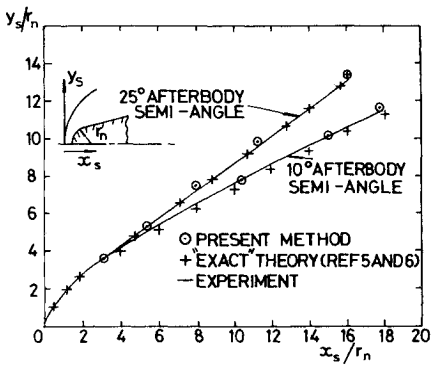

Fig. 2 Shock wave profiles for spherically blunted cones ($M=2.50$).

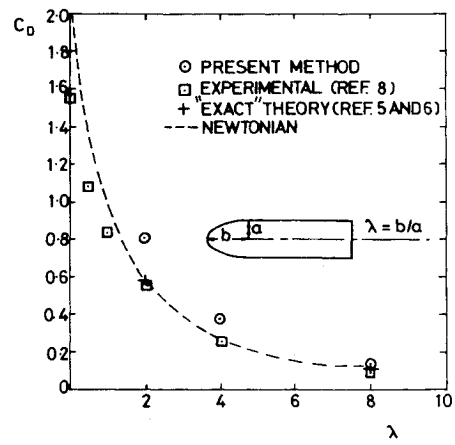

Fig. 4 Drag of elliptically blunted cylinders ($M=2.50$).

Acknowledgment

The author wishes to acknowledge the financial support given to this work by the ministry of Defence, U.K., and to P.G. Pugh of RAE, Bedford, U.K. for many helpful discussions.

References

[1] Pugh, P.G. and Ward, L.C., "A Novel Method for the Estimation of Zero Lift Forebody Drag of Axisymmetric Non-Slender Shapes at Supersonic and Hypersonic Velocities," Aeronautical Research Council, CP 1142, 1971.

[2] Oswatitsch, K. and Kuerti, G., *Gas Dynamics,* Academic Press, New York, 1956, p. 203.

[3] Kaattari, G., "A Method of Predicting Shock Shapes and Pressure Distributions for a Wide Variety of Blunt Bodies at Zero Angles of Attack," NASA TN D-4539, 1968.

[4] Philpott, D.R., "A Simple Flow Model for the Calculation of the Flow Round a Blunt Axisymmetric Body at Supersonic Speeds," AIAA Paper No. 78-1356, 1978.

[5] Albone, C.M., "Blunt Body Flows at Supersonic Speeds," City University Research Report 71/1, 1971.

[6] Philpott, D.R., " A Program for the Calculation of Axisymmetric Supersonic Flows around Blunt Bodies using a Reference Plane Method," The Hatfield Polytechnic, THP/4-73R, 1973.

[7] Engineering Sciences Data Unit (Royal Aeronautical Society), Engineering Sciences Data Item 68021, 1968.

[8] Philpott, D.R., "An Investigation into the Flow around a Family of Elliptically Nosed Cylinders at Zero Incidence at $M=2.50$ and $M=4.00$," *Aeronautical Quarterly,* Vol. XXIII, Nov. 1972.

NA

J80-024

20004

Resonant Wave Interactions on a Swept Wing

Spyridon G. Lekoudis*
Lockheed-Georgia Company, Marietta, Ga.

Introduction

EXPERIMENTS on the growth of laminar instabilities in a Blasius boundary layer[1] show that near the end of the region of the linear growth of the two-dimensional Tollmien-Schlichting wave a three-dimensional pattern appears. The exact position and form of this pattern is a matter of controversy because more recent experiments[2] show that the three dimensionality is random with no distinguishable spanwise wavelength.

One of the analytical models that has been proposed to explain the three-dimensionality of the Blasius layer is resonant wave interactions. Craik[3] examined the pattern consisting of a two-dimensional Tollmien-Schlichting wave and two oblique waves symmetric about the flow direction. The oblique waves had half the frequency of the two-dimensional wave. The rapid growth of the oblique waves is explained by the rapid transfer of energy from the mean flow to the oblique waves.[3] The model has been re-examined by Lekoudis[4] using spatial stability theory, but no calculations were performed. Calculations of the amplitudes of resonant triads have been performed by Volodin and Zel'man.[5] They used Craik's model in a Blasius boundary layer and predicted rapid growth of the amplitudes of all the interacting waves; however, they also showed that the initial phasing and the spanwise periodicity could act as detuning and lessen the strength of the interaction. Nayfeh and Bozatli calculated the result of the modification of the Blasius layer from a Tollmien-Schlichting wave of large amplitude,[6] and examined nonlinear wave interactions using the resonance model.[7] They found that a rapid increase of the oblique waves can occur. They also found that the strength of the interaction is proportional to the initial amplitude of the waves.

Recent flat plate vibrating ribbon experiments[2] show the subharmonic growing in a region of Reynolds numbers where linear theory predicts it should decay. The same kind of experiments show the growth to be dependent on the initial conditions.[8] Moreover, another set of recent experiments[9] examined the evolution of the spectrum in a Blasius boundary layer excited by two vibrating ribbons. The spectrum is filled with frequencies that are combinations of the two excitation frequencies. This behavior can be explained by a generalization of the resonance model.

Next, the theory is extended to the case of three-dimensional boundary-layer flows, and applied to the case of the boundary layer on a transonic swept wing with laminar flow control.

Formulation of the Problem

We consider the nonlinear stability of a three-dimensional boundary-layer flow on a swept wing with laminar flow control. The Cartesian coordinate system used has the x axis in the direction of normal chord, the y axis normal to the surface, and the z axis along the span.

We assume a locally parallel, three-dimensional boundary-layer flow consisting of a steady mean part and an unsteady disturbance part. The disturbance part consists of wave triads:

$$\begin{Bmatrix} \tilde{u} \\ \tilde{v} \\ \tilde{w} \\ \tilde{p} \end{Bmatrix} = \epsilon \sum_{j=0}^{2} A_j(\epsilon x, \epsilon z, \epsilon t) \begin{Bmatrix} u_j(y) \\ v_j(y) \\ w_j(y) \\ p_j(y) \end{Bmatrix} \exp(i\theta_j) \tag{1}$$

where ϵ is a small number characteristic of the weak nonlinearity of the system we are examining, u, v, and w denote the velocity components in the x, y, and z directions, respectively, p is the pressure, and the tildes denote disturbance quantities. Also,

$$\theta_j = \alpha_j x + \beta_j z - \omega_j t \qquad j=0,1,2 \tag{2}$$

In Eq. (2), α_j and β_j are the wavenumbers in the x and z directions, respectively, and ω_j are frequencies. In Eq. (1), A_j is the slowly varying amplitude. We introduce the slow scales[10]

$$X=\epsilon x \qquad Z=\epsilon z \qquad T=\epsilon t \tag{3}$$

Substituting Eqs. (1-3) into the incompressible Navier-Stokes equations, linearizing and separating harmonics, we find that the disturbance is governed to first order in ϵ by the Orr-Sommerfeld problem for the case of a three-dimensional boundary layer. In order for the waves to satisfy resonance conditions, we require that

$$\theta = \theta_1 + \theta_2 - \theta_0$$

$$\frac{\partial\theta}{\partial x} = O(\epsilon) \quad \frac{\partial\theta}{\partial z} = O(\epsilon) \quad \frac{\partial\theta}{\partial t} = O(\epsilon) \tag{4}$$

Using Eq. (4) and applying solvability conditions to the $0(\epsilon^2)$ equations, we arrive at the following quasilinear, first-order, partial differential equations that govern the slowly varying

Received March 27, 1979; revision received Aug. 6, 1979. Copyright © American Institute of Aeronautics and Astronautics, Inc., 1979. All rights reserved.

Index category: Boundary-Layer Stability and Transition.

*Consultant. Member AIAA.